JLab PAC12 Proposal Cover Sheet

This document must be received by close of business on June 26, 1997

Jefferson Lab
User Liaison Office, Mail Stop 12 B
12000 Jefferson Avenue
Newport News, VA 23606

(Choose one)

☒ New Proposal Title: Spectroscopic study of Λ hypernuclei beyond the p-shell region through the (e,e'K^+) reaction

☐ Update Experiment Number:

☐ Letter-of-Intent Title:

Contact Person

Name: Osamu Hashimoto
Institution: Tohoku University
Address: Department of Physics
Address: Tohoku University
City, State, ZIP/Country: Sendai, 980-77, Japan
Phone: 81-22-217-6452 Fax: 81-22-217-6455
E-Mail: Hashimot@lambda.phys.tohoku.ac.jp
Local contact: R. Sawafta, sawafta@CEBAF.GOV, Ext:7353, or
L. Tang, tangl@CEBAF.GOV, Ext:6255

Experimental Hall: C Days Requested for Approval: 35

Jefferson Lab Use Only

Receipt Date: 6/26/97 97-008

By:

HAZARD IDENTIFICATION CHECKLIST

JLab Proposal No.: _____ Date: _____
(For CEBAF User Liaison Office use only.)

Check all items for which there is an anticipated need.

Cryogenics N/A
_____ beamline magnets
_____ analysis magnets
_____ target
type: _____
flow rate: _____
capacity: _____

Electrical Equipment N/A
_____ cryo/electrical devices
_____ capacitor banks
_____ high voltage
_____ exposed equipment

Radioactive/Hazardous Materials
List any radioactive or hazadorous/ toxic materials planned for use:
N/A

Pressure Vessels
_____ inside diameter
_____ operating pressure
_____ window material
_____ window thickness

N/A

Flammable Gas or Liquids
type: _____
flow rate: _____
capacity: _____

Drift Chambers
type: Ethane (SOS)
flow rate: Standard (SOS)
capacity: Standard (SOS)

Other Target Materials
___ Beryllium (Be)
___ Lithium (Li)
___ Mercury (Hg)
___ Lead (Pb)
___ Tungsten (W)
___ Uranium (U)
X Other (list below)
Si and V

Vacuum Vessels N/A
_____ inside diameter
_____ operating pressure
_____ window material
_____ window thickness

Radioactive Sources N/A
_____ permanent installation
_____ temporary use
type: _____
strength: _____

Large Mech. Structure/System
X lifting devices
_____ motion controllers
_____ scaffolding or
_____ elevated platforms
If HNSS has to be re-instal ex

Lasers N/A
type: _____
wattage: _____
class: _____

Installation:
_____ permanent
_____ temporary

Use:
_____ calibration
_____ alignment

Hazardous Materials N/A
___ cyanide plating materials
___ scintillation oil (from)
___ PCBs
___ methane
___ TMAE
___ TEA
___ photographic developers
___ other (list below)

General:

Experiment Class:

_____ Base Equipment
_____ Temp. Mod. to Base Equip.
_____ Permanent Mod. to Base Equipment
_____ Major New Apparatus

Other: Same as E89-009

BEAM REQUIREMENTS LIST

Lab Proposal No.: _____ Date: _____

Hall: C Anticipated Run Date: 1999 PAC Approved Days: _____

Spokesperson: O.Hashimoto/L.Tang/R.Sawafta
Hall Liaison: R. Carlini
Phone: 81-22-217-6452/269-6255/269-7353
E-mail: Hashimot@lambda.phys.tohoku.ac.jp
tangl@cebaf.gov
sawafta@cebaf.gov

List all combinations of anticipated targets and beam conditions required to execute the experiment. (This list will form the primary basis for the Radiation Safety Assesment Document (RSAD) calculations that must be performed for each experiment.)

Condition No.	Beam Energy (MeV)	Mean Beam Current (μA)	Polarization and Other Special Requirements (e.g., time structure)	Target Material (use multiple rows for complex targets — e.g., w/windows)	Material Thickness (mg/cm²)	Est. Beam-On Time for Cond. No. (hours)
1	1645	0.8	N/A	^{28}Si	10mg/cm2	300*
2	1645	0.6	N/A	^{51}V	10mg/cm2	540*
* 60 hours of beam-on target tuning and calibration are included for each target.						

The beam energies, E_{Beam}, available are: $E_{Beam} = N \times E_{Linac}$ where N = 1, 2, 3, 4, or 5. E_{Linac} = 800 MeV, i.e., available E_{Beam} are 800, 1600, 2400, 3200, and 4000 MeV. Other energies should be arranged with the Hall Leader before listing.

Version June 26, 1997

Spectroscopic study of Λ hypernuclei beyond the p-shell region through the (e,e'K$^+$) reaction

O. Hashimoto(Spokesperson)*, K. Maeda, K. Suda, T. Takahashi, H. Tamura, Y. Sato

Department of Physics, Tohoku University, Sendai, 980-77, Japan

T. Endo

Laboratory for Nuclear Science, Tohoku university, Sendai, 982, Japan

H. Noumi

Institute for Particle and Nuclear Physics, KEK, Tsukuba, 305, Japan

T. Motoba

Laboratory of Physics, Osaka Electro-Communication University, Neyagawa, 572, Japan

L. Tang(Spokesperson), K. Assamagan, O.K. Baker, P. Gueye, C. Keppel, L. Yuan

Department of Physics, Hampton University, Hampton, VA 23668, USA

R. Sawafta(Spokesperson), S. Beedoe, S. Danagoulian, C. Jackson, S. Mtingwa

Department of Physics, North Carolina A& T State University, Greensboro, NC 27411 USA

M. Ahmed, R. Barber, A. Empl, E. Hungerford, K. Lan, B. Mayes, L. Pinsky, J. Wilson

Department of Physics, University of Houston, Houston, TX 77204 USA

R. Carlini, T. Eden, R. Ent, J. Mitchell, W. Vulcan, S. Wood, C. Yan

Thomas Jefferson National Accelerator Facility, Newport News, VA 23606 USA

M. Elaasar, D. Greenwood, K. Johnston, N. Simicevic, S. Wells

Department of Physics, Louisiana Tech University, Ruston, LA USA

J.C. Martoff

Department of Physics, Temple University, Philadelphia, PA USA

R. Chrien, M. May, A. Rusek
Brookhaven National Laboratory, Upton, NY USA

T. Amatouni, H. Mkrtchyan, A. Margaryan, V. Tadevosyan
Yerevan Physics Institute, Armenia

D. Androic, M. Planinic, D. Bosnar, M. Furic
Department of Physics, University of Zagreb, Croatia

T. Angelescu, A. Mihul
Department of Physics, University of Bucharest, Romania

June 26, 1997

* Contact person

Osamu Hashimoto
Department of Physics, Tohoku University, Sendai, 980-77, Japan
hashimot@lambda.phys.tohoku.ac.jp
Telephone 81-22-217-6452
Telefax 81-22-217-6455

Proposal to JLAB PAC-12

Abstract

We propose to perform a spectroscopic study of Λ hypernuclei beyond the p shell region with the best possible resolution, and to determine the spin-orbit potential of Λ hypernuclei in ${}^{28}_{\Lambda}$Al and ${}^{51}_{\Lambda}$Ti. The approved experiment E89-09 which is under preparation intends to establish high resolution spectroscopy of Λ hypernuclei in the p shell region by the (e,e'K$^+$) reaction. The present proposal is to extend the spectroscopy to the heavier targets such as ^{28}Si and ^{51}V with emphasis on revealing the spin-orbit interaction of a Λ hyperon in medium heavy nuclei.

Although experiments become difficult in the high Z region because of bremsstrahlung in the target, experiment E89-09 can be extended in a straightforward way up to the mass 50 region. By achieving sub-MeV energy resolution (around 600 keV), we will obtain quality hypernuclear spectra with the best energy resolution to date, and will reveal the structure of Λ hypernuclei beyond the p shell region. By using ^{28}Si and ^{51}V targets we will study the spectra of the ${}^{28}_{\Lambda}$Al and the ${}^{51}_{\Lambda}$Ti hypernuclei, respectively. The ls-splitting of Λ hyperon orbitals is expected to be greater in these heavier Λ hypernuclei, providing an opportunity to determine its magnitude. We propose to take advantage of the following unique characteristics of Jefferson Laboratory (JLAB):

- The (e,e'K$^+$) reaction favorably excites both spin-flip and non-spin-flip high spin states.
- JLAB offers the best opportunity for the reaction spectroscopy of Λ hypernuclei with sub-MeV resolution.

We also intend to shed light on the current puzzling situation of the ΛN ls interaction and to investigate the structure of Λ hypernuclei beyond the p shell region in a qualitative way.

1 Introduction

Nuclear systems with strangeness -1 provide a unique opportunity to investigate new forms of nuclei and new aspects of the strong and weak interactions in nuclear medium. Particularly, recent progress in experimental studies of Λ hypernuclei has opened a new pathway towards understanding nuclear systems with strangeness in a quantitative way.

A Λ hyperon survives long enough to form Λ hypernuclear states which are narrow enough to be observed as individual peaks, making it possible to conduct spectroscopic investigations. Bound states of Λ hypernuclei decay electromagnetically or by the weak interaction, so that the widths of such states are narrow. Even when considering the structure of these levels as particle-hole excitations, the spreading widths have been calculated to be less than a few 100 keV [1, 2]. This is due to the following reasons.

- The Λ isospin is 0 and only isoscaler particel-hole modes of the core nucleus are excited.
- The ΛN interaction is much weaker than the nucleon-nucleon interaction.
- The ΛN spin-spin interaction is weak and therefore the spin vector p_N-h_N excitation is suppressed.
- There is no exchange term.

As a result, particle-hole Λ hypernuclear states are much narrower than that of ordinary nuclei for the states of the same excitation energy. In the case of Ca for example, it was predicted that $\Gamma_\Lambda(1s \text{ or } 0d)/\Gamma_N(0s) = 0.03\text{-}0.07$, resulting in a spreading width narrower than a few hundred keV even for the excited states above the particle emission threshold. This gives a sound basis for spectroscopic studies of heavy Λ hypernuclei. Spectra have already been demonstrated experimentally for a wide range of nuclei via many reactions, but the (e,e′K^+) reaction still offers the best hope for a quantitative advance in this field due to its nature and its potential to achieve high resolution.

2 Hypernuclear structure and ΛN interaction

Although there are some experiments and proposals to directly measure hyperon-nucleon scattering, the data are limited and of poor quality. Such experiments require hyperon beams and are extremely difficult, particularly those measuring spin dependent parameters. Spectroscopic investigations of Λ hypernuclei, therefore, play a vital role in the extraction of the bare interaction from the effective hyperon-nucleon interaction. These investigations are particularly important to determine the spin dependent terms, complementing the scattering experiments. The weakness of the interaction between a Λ hyperon and the rest of the nuclear system allows one to reliably extract information on the interaction from the structure data.

Starting from the phenomenological YN and YY interactions [3, 4], which are constructed based on limited scattering data of hyperons, and further assuming flavor SU(3) symmetries, a YN and YY effective interaction in finite nuclei [5] was derived as a YN G potential in the three-range gaussian form,

$$v_{\Lambda N}(r) = \sum^{3}(a_i + b_i k_F + c_i k_F^2) exp(-r^2/\beta_i^2).$$

With this analytical potential, hypernuclear properties such as hyperon binding energies, excitation energies, cross sections, polarization, and weak decay widths, etc. can be calculated. Thus experimental data on hypernuclei can be directly compared with the calculated properties based on this ΛN potential.

In a more phenomenological approach, the effective interaction in the p-shell Λ hypernuclei is usually parametrized as,

$$V_{\Lambda N}(r) = V_0(r) + V_\sigma(r) s_N \cdot s_\Lambda + V_\Lambda(r) l_{\Lambda N} \cdot s_\Lambda + V_N(r) l_{\Lambda N} \cdot s_N + V_T(r) S_{12}$$

where $S_{12} = 3(\sigma_N \cdot \hat{r})(\sigma_\Lambda \cdot \hat{r})/r^2 - \sigma_n \cdot \sigma_\Lambda$ [6, 7]. In the p-shell there is one radial integral for each term, which is then parametrized by the factors; Δ, S_N, S_Λ and T. In the papers referenced above, the determination of these parameters was based on the data then available, that is;

1. the upper limit of the the spin-orbit splitting determined from the (K^-, π^-) reaction spectra for $^{13}_{\Lambda}C$;
2. the failure to resolve the p-orbital spin-orbit partner of $^{9}_{\Lambda}Be$ in the $p_\Lambda \rightarrow s_\Lambda$ transition, and;
3. the M1 γ ray energies between the spin-flip partner states of $^{4}_{\Lambda}H$ and $^{4}_{\Lambda}He$.

The parameters were deduced to be Δ = 0.5 MeV, S_Λ = -0.04 MeV,S_N = -0.08 MeV and T = 0.04 MeV [7]. Later Fetisov *et al.* updated this set of parameters by taking into account a newer data set which included an upper limit on the ground state doublet splitting in $^{10}_{\Lambda}B$ and $^{16}_{\Lambda}O$ and the spin-parity assignments in the p-shell. However this analysis ignored the ground state binding energies and the value of the spin-spin parameter extrapolated from the s-shell. They obtained the parameter set; Δ = 0.25 MeV, S_Λ = -0.02, S_N = -0.2 and T = 0.04 [8]. These parameters of the phenomenological ΛN interaction are experimentally determined through the structure information of Λ hypernuclei.

However there are both experimental and theoretical reasons why one might expect that a universal parameter set could not be defined. Theoretically the ΛNN three-body force is important because of the large ΛN→NN conversion. This naturally introduces a three-body force through intermediate coupling to the Σ hyperon, and one notes that the long range OPE, while excluded in the ΛN interaction, must be included in the $\Lambda \rightarrow \Sigma$ conversion potential. Experimentally it is well known that a repulsive three-body force is required to fit the s-shell hypernuclear levels when using an effective ΛN potential. These interactions are spin-isospin dependent, contrary to the assumptions of the original parameterization.

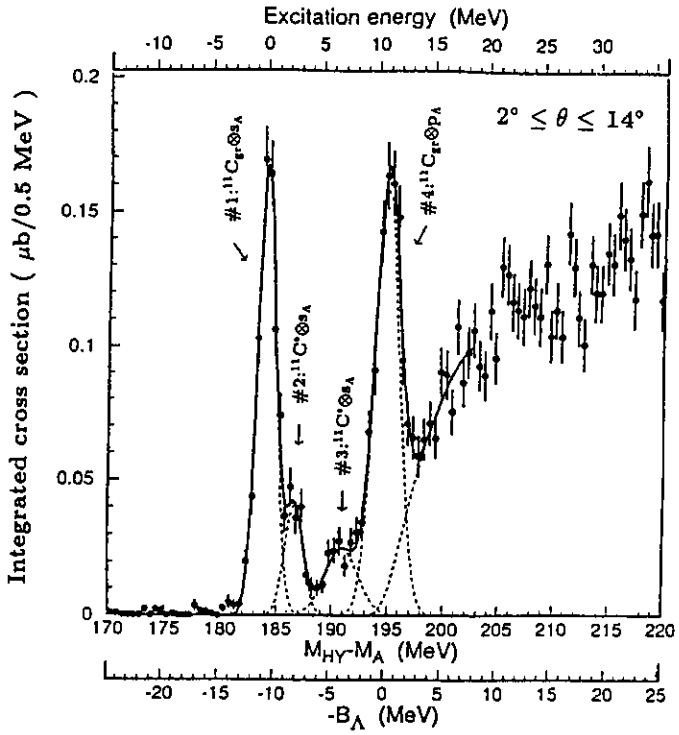

Figure 1: Excitation spectrum of ${}^{12}_{\Lambda}$C obtained by ^{12}C$(\pi^+,\mathrm{K}^+)^{12}_{\Lambda}$C reaction with the INS-SKS spectrometer system, showing the energy resolution of 2 MeV(FWHM).

The importance of good resolution Λ hypernuclear spectroscopy has been recently demonstrated through the ${}^{12}_{\Lambda}$C spectrum by the (π^+, K^+) reaction with 2 MeV resolution, spectrum of which is shown in Fig.1. The KEK experiment clearly observed two satellite peaks between the two prominent ones which were identified as having configurations of $\nu p_{3/2}^{-1} \otimes \Lambda s_{1/2}$ and $\nu p_{3/2}^{-1} \otimes \Lambda p_{1/2,3/2}$ [9]. The smaller peaks carry about 1/10 of the cross section of the more prominent ones, and were interpreted as states constructed from an $s_{1/2}$ Λ hyperon coupled to excited states of the ^{11}C core. This is the first time that the core excited Λ hypernuclear states were observed. Comparison of the calculation based on the phenomenological ΛN interaction to these cross sections, and the excitation energies have been discussed in favor of a stronger spin singlet interaction.

This is an encouraging example that demonstrated the importance of precision Λ hypernuclear spectroscopy in investigating the hyperon-nucleon interaction. The approved E89-09 experiment under preparation addresses these investigation in the p shell region.

3 Spin-orbit splitting of Λ hypernuclear states

It has been assumed for a long time that the Λ spin-orbit splitting is very small in contrast to the nucleon case. Comparison of ${}^{12}_{\Lambda}$C and ${}^{16}_{\Lambda}$O spectra by the (K^-, π^-) reaction at CERN gave the strength of the spin-orbit potential to be $V_{so} = 2 \pm 1$ MeV [10, 11].(In this proposal, the convention of reference [29] is used.) Later, the angular distribution of the ^{13}C$(\mathrm{K}^-,\pi^-)^{13}_{\Lambda}$C reaction was measured at BNL, and an even smaller value was reported [12]. Detail analysis of emulsion ${}^{12}_{\Lambda}$C data claimed the observation of two peaks which can be attributed as members of spin-orbit

Table 1: Theoretical prediction of the spin-orbit potential

Theory	V_{so}^{N}	V_{so}^{Λ}	V_{so}^{Σ}	comment
Mean field theory	1	0.04	0.7	Bouyssy[14]
Meson exchange model	1	0.25	0.5	Brockmann[15, 16]
Additive quark model	1	0	4/3	Pirner[17]
Nonrelativistic quark cluster model	1	0.21	0.55	Morimatsu[18]
One-boson-exchange	1	0.19-0.26	0.27-0.40	Dover[19]

splitting [13]. The width of the Λ p-shell peak in the new $^{12}_{\Lambda}$C spectrum by the (π^+, K^+) reaction was also consistent with the emulsion analysis [9].

The small spin-orbit potential is inherited from the small elementary ΛN spin-orbit interaction. Many theoretical attempts have succeeded in explaining the small size of the spin-orbit interaction, but absolute magnitudes vary from model to model as summarized in Table 1. A simple constituent quark model, for example, gives exactly zero spin-orbit coupling, while a meson exchange model yields a finite value.

Since the spin-orbit interaction has a short-ranged nature, an experimental value of the spin-orbit splitting provides key information on ΛN interaction. Although it has been widely accepted that the spin-orbit splitting is too small to be directly observed in experiment, arguments based on two different approaches were given recently, suggesting that the spin-orbit parameter should have a larger value. Dalitz *et al.* made a detail analysis of $^{16}_{\Lambda}$O emulsion data, and claimed that the energy splitting of 0^+ and 2^+ states, which are spin-orbit partners of $p_{3/2}$ and $p_{1/2}$ Λ hyperons, is around 1.5 MeV. This splitting is considerably larger than previously believed [20]. It was also claimed that the excitation energy spectrum of the $^{89}_{\Lambda}$Y, which was obtained by the (π^+, K^+) reaction with 2.2 MeV resolution, can be better reproduced, if a 2-3 times larger spin-orbit potential than the ordinary value is assumed, particularly for high-l Λ orbitals [21]. On the other hand, in a recent E336 experiment with the SKS spectrometer at KEK-PS, a high-quality $^{16}_{\Lambda}$O excitation energy spectrum by (π^+, K^+) reaction was measured as shown in Fig.2 [22]. The reaction preferentially excite the 2^+_1 state, as compared to the 0^+_1 state which would be excited by the recoilless (K^-, π^-) reaction which favors substitutional states. The energy splitting of the two states strongly reflects the spin-orbit interaction. As can be seen in the figure, the present spectrum, with good resolution and statistics, give an excitation energy of the 2^+_1 state. Using the excitation energy spectrum of the 0^+_1 state from the CERN (K^-, π^-) reaction data [10, 20], the energy difference of the two states is derived to be very small, in contradiction with the above

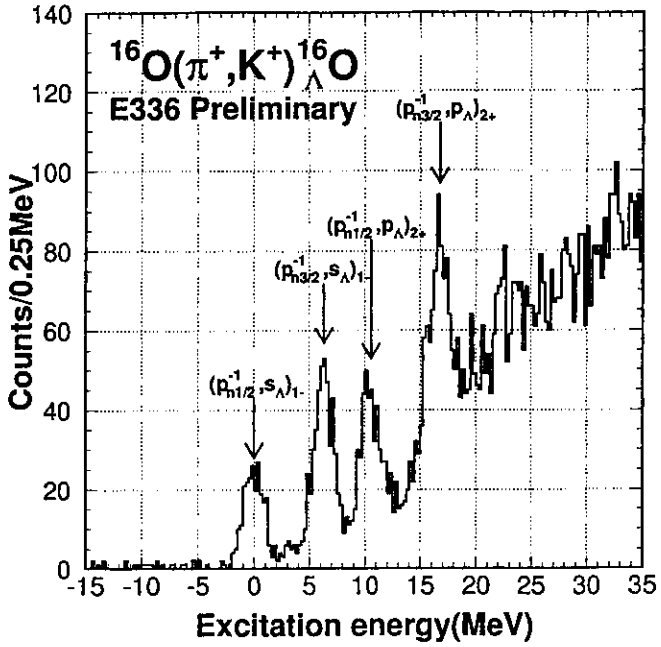

Figure 2: Preliminary excitation spectrum of $^{16}_{\Lambda}O$ obtained by $^{16}O(\pi^+,K^+)^{16}_{\Lambda}O$ reaction with the INS-SKS spectrometer system.

suggestions of a larger spin-orbit splitting [22].

The investigation of the spin-orbit interaction in Λ-nucleon system is one of the key issues in strangeness nuclear physics, but the experimental situation is still quite puzzling. It can be clarified only by high resolution experiments. The (e,e'K$^+$) reaction at JLAB offers one of the best opportunities for directly observing the splitting with sub-MeV energy resolution. This is the motivation for the present proposal, and will be described in detail in section 5.

It should also be mentioned that there is an effort to conduct Λ hypernuclear spectroscopy through gamma ray measurements of Λ hypernuclei. With gamma detectors such as Ge or NaI, it is possible to achieve a few to several ten's keV energy resolution. This is 2-3 orders of magnitude better than that which could be obtained from reaction spectroscopy. For example, the 10 MeV gamma ray between the $p_{1/2}\Lambda$ to the $s_{1/2}\Lambda$ ground state has been observed at BNL with NaI [23]. There is an approved BNL experiment that intends to measure the coincident γ transitions between the p and s orbitals of $^{13}_{\Lambda}C$, and to determine the splitting of $p_{1/2}$ and $p_{3/2}$ states [24].

However, the study of γ spectra coincident with hypernuclear events are not trivial, suffering from low statistics. Furthermore and more importantly, the separation of true hypernuclear gammas from coincident nuclear transitions is often ambiguous. In addition, studies of γ emitting hypernuclear states are limited to some p orbitals in light Λ hypernuclei because of particle emission. Therefore, high resolution reaction spectroscopy and γ spectroscopy of Λ hypernuclei are complimentary to each other.

Table 2: Comparison of Λ Hyperon production reactions

$\Delta Z = 0$ *neutron to* Λ	ΔZ = -1 *proton to* Λ	comment
(π^+, K^+)	(π^-, K^0)	stretched,high spin
in-flight (K^-, π^-) stopped (K^-, π^-)	in-flight (K^-, π^0) stopped (K^-, π^0)	substitutional
$(e, e'K^0)$ (γ, K^0)	$(e, e'K^+)$ (γ, K^+)	spin-flip,unnatural parity

4 The (e,e'K$^+$) vs. (π^+,K$^+$) vs. (K$^-$,$\pi^{-,0}$) reactions

A wide variety of reactions can be used to produce a strangeness -1 hyperon as listed in Table 2. Each reaction has its own characteristics which plays significant role in selectively populating Λ hypernuclear states. Among them, only the (K^-, π^-) and (π^+, K^+) reactions have been used to date. These reactions convert a neutron in the target to a Λ hyperon. Although the (π^+, K^+) reaction is relatively new compared to the (K^-, π^-) reaction, it is now considered as one of the best reactions to populate deeply bound hypernuclear states [25, 9, 26]. The smaller cross sections of the (π^+,K$^+$) reaction compared to that of the (K$^-$,π^-) reaction is compensated by the availability of more intense pion beams. The (π^+,K$^+$) reaction selectively populates angular momentum stretched states because of the large momentum transfer to the recoil hypernuclei [27, 28, 29]. This is in contrast to the (K^-, π^-) reaction which transfers small momentum and accordingly preferentially excites substitutional states.

A superconducting kaon spectrometer (SKS), which has a good momentum resolution of 0.1 % as well as a large solid angle of 100 msr in the 1 GeV/c region, has been utilized for Λ hypernuclear spectroscopy by the (π^+, K^+) reaction at KEK 12 GeV PS [30, 31]. An intensive spectroscopic study of Λ hypernuclei has been carried out with this spectrometer. Binding energies of a Λ hyperon in a nucleus as heavy as Pb have been extracted from the spectra and the central part of the Λ hyperon potential was experimentally investigated [26, 32]. It was possible to qualitatively discuss the characteristics of the Λ-nucleon interaction through the good resolution (2 MeV FWHM) spectra of the light hypernuclei as mentioned in section 2.

At BNL, a high resolution π^0 spectrometer has been recently installed and the experiment is under way [33]. High quality spectroscopy of the *p*-shell Λ hypernuclei with resolution around 1 MeV will be realized by the use of the π^0 spectrometer. In this reaction, a proton is converted to a Λ hyperon, similar to the (e,e'K$^+$) reaction.

In contrast to these reactions, the electromagnetic reactions have an advantage in

populating the spin-flip hypernuclear states. Since the (π^+, K^+) and (e,e'K^+) reactions transfer almost the same recoil momentum, the two reactions have a similar characteristics in that they populate high-spin bound hypernuclear states. However, the most significant difference between the two reactions is that the (e,e'K^+) reaction favorably excites spin-flip states as well as non-spin-flip states. The transition operator of electromagnetic production of a hyperon has spin-independent(f) and spin-dependent(g) terms [34]. Although the spin independent term is significantly smaller than the spin-dependent term, the spin-flip and non-spin-flip parts in the spin-dependent term have amplitudes comparable to each other. Therefore, in the (e,e'K^+) reaction, both natural-parity and unnatural-parity states are excited in contrast to hypernuclear production reactions with meson beams such as (K^-, π^-) and (π^+, K^+) reactions. This selectivity is particularly useful as it simplifies the resulting spectra. We will explain this again for the ^{28}Si(e,e'K^+)$^{28}_{\Lambda}$Al reaction in Section 5. Also the (e,e'K^+) reaction has possibility of achieving significantly better energy resolution, because it utilizes a primary beam with extremely good beam emittance contrary to secondary beams.

The study of hypernuclear spectra produced by many different reactions which have unique characteristics, is of vital importance to sort out the structure of the excited hypernuclear levels. With this in mind, a collaborative program to link the three efforts for Λ hypernuclear spectroscopy involving the (π^+, K^+) reaction at KEK 12 GeV-PS, (K^-, π^-) reaction at BNL AGS, and (e,e'K^+) reactions at JLAB is underway.

5 Physics goal of the proposed experiment

In the present proposal, we use the fact that the HNSS in Hall C will achieve sub-MeV energy resolution. We choose targets which have relatively large spin-orbit splittings compared to those in the p shell region, so that we have a better chance to directly observe the splitting in a Λ hypernucleus. This is meaningful only by using the (e,e'K^+) reaction, since the experimental resolution is possibly better than the magnitude of ls splitting. The magnitude of the spin-orbit splitting is proportional to the derivative of the Λ potential, the strength of the spin-orbit potential(V_{so}), and $l_\Lambda(l_\Lambda + 1)$. The magnitude of the splitting for a given Λ orbital was calculated assuming $V_{so} = 2.0$ MeV [35] and is illustrated in Fig.3. As seen in the figure, the splitting takes its largest value around a hypernuclear mass of 20-30 for the p orbital and around 40-50 for the d orbital. The splitting is expected to be about 1.2 MeV for the p orbital of $^{28}_{\Lambda}$Al and 1.3 MeV for $^{51}_{\Lambda}$Ti when $V_{so} = 2.0$ MeV. Larger spin-orbit splitting is expected in the mass region heavier than the p-shell. By the (e,e'K^+) reaction with energy resolution of 600 keV, we will resolve the splitting smaller than 1 MeV. Even if V_{so} is half the assumed value, the splitting should be observed.

In order to help resolve the puzzle of the ΛN spin-orbit interaction as described in Section 3, we propose a high-resolution spectroscopic investigation of two targets, in an attempt to resolve the spin-orbit partners. Each reaction is described below.

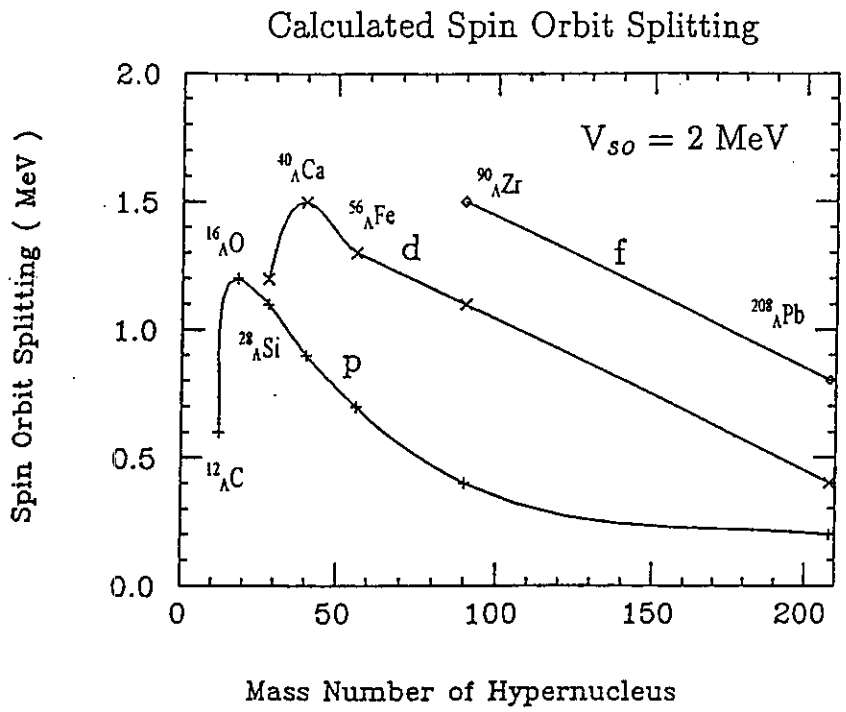

Figure 3: Calculated spin-orbit splitting as a function of Λ hypernuclear mass number [35].

^{28}Si(e,e'K$^+$)$^{28}_{\Lambda}$Al reaction :

It has been shown the *ls* splitting of the *p*-orbital reaches almost a maximum around Si as seen in Fig.3.

The ^{28}Si(π^+,K$^+$)$^{28}_{\Lambda}$Si reaction was studied using the SKS spectrometer with 2 MeV resolution, a spectrum of which is shown in Fig.4 [26]. Although we see the *p* orbital peak at about B_Λ = 7 MeV, the *ls* splitting was not observed.

However, sub-MeV resolution spectroscopy which will be realized at JLAB will provide the best opportunity to directly measure the *ls* splitting. Even if the spin-orbit splitting is smaller than the resolution, we will be able to set a stringent limit on its magnitude.

The excitation energy spectrum for the (γ,K$^+$) reaction has been calculated at E_γ = 1.30 GeV and θ_K = 3 degrees, which are similar kinematical conditions of the proposed (e,e'K$^+$) reaction on a Si target at E_e = 1.645 GeV. In the present setup of the Hall C HNSS, the energy of the virtual photon is 1.36 GeV and the kaons are detected at 3 degrees. The spectrum in Fig.5 was obtained assuming the V_{so} is 2 MeV and has been folded with the expected energy resolution of 600 keV(FWHM). Deep proton hole states such as $p^{-1}_{1/2}$ and $p^{-1}_{3/2}$ are assumed to have 4 MeV spreading width. The calculation showed that the reaction strongly favors excition of the highest spin-states for a given Λ particle-proton hole configuration. For a Λ hyperon in the *p* orbital, $[\pi d^{-1}_{5/2} \otimes \Lambda p_{3/2}]4^-$ and $[\pi d^{-1}_{5/2} \otimes \Lambda p_{1/2}]3^-$ states are dominantly populated, providing a good opportunity to directly observe the *ls* splitting. Figure 5 clearly demonstrates possibility to observe the splting.

In the case of the (π^+, K$^+$) reaction, the excitation spectrum was calculated with the full shell-model wave-functions in the *sd* shell space although the calculation for the ^{28}Si(e,e'K$^+$)$^{28}_{\Lambda}$Si reaction will be completed in the near future.

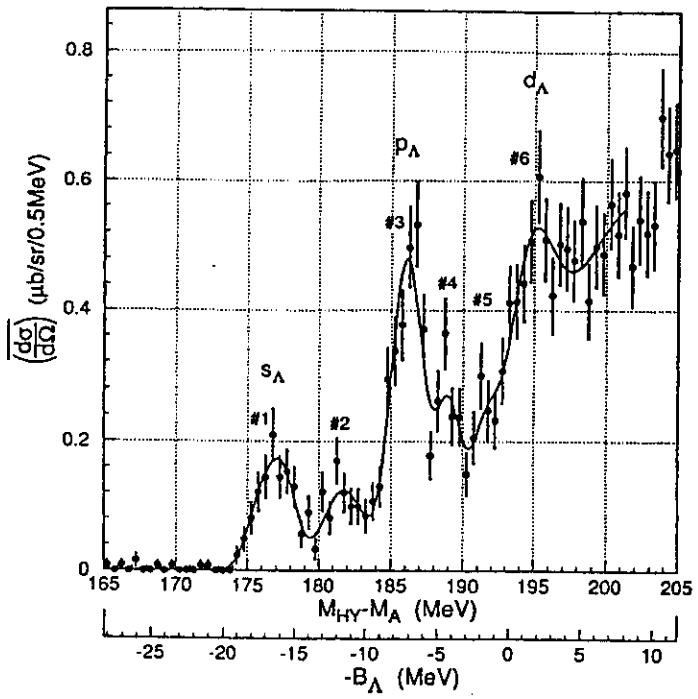

Figure 4: Excitation spectrum of ${}^{28}_{\Lambda}$Si obtained by ^{28}Si(π^+,K$^+$)${}^{28}_{\Lambda}$Si reaction with the SKS spectrometer system. Energy resolution is 2 MeV(FWHM) [26].

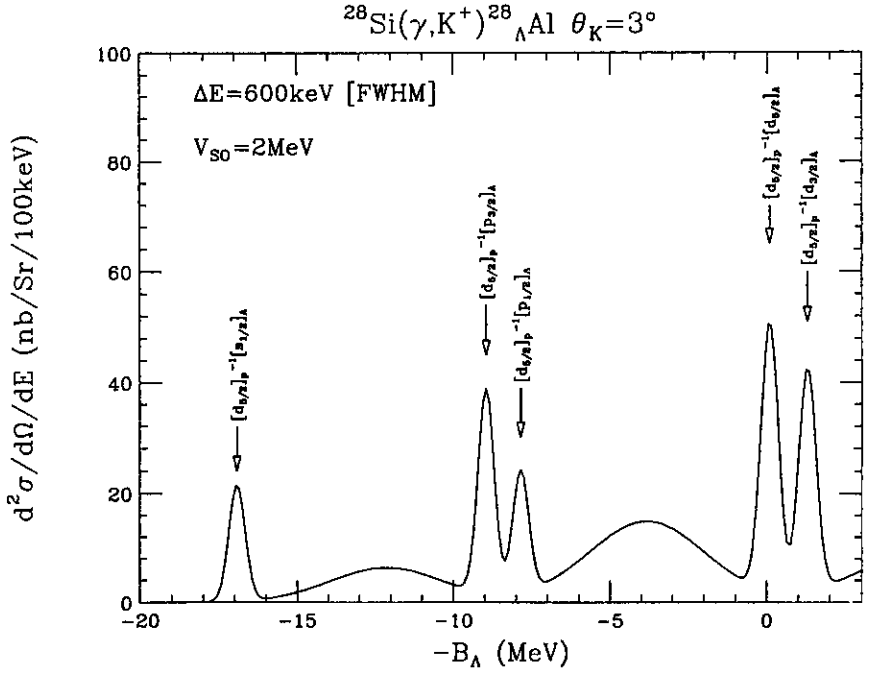

Figure 5: Calculated excitation function of ^{28}Si(γ,K$^+$)${}^{28}_{\Lambda}$Al reaction at E_γ = 1.3 GeV/c and θ_K = 3 deg [37]. Spin-orbit splitting of the p and d orbitals is assumed to be 1.1 and 1.2 MeV respectively as taken from Fig.3. Contribution from p proton-hole states are smeared by 4 MeV.

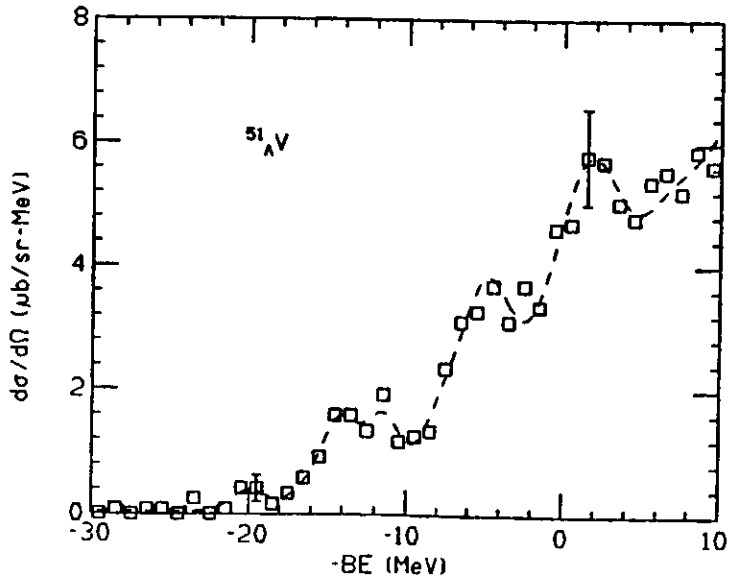

Figure 6: Excitation spectrum of $^{51}_{\Lambda}$V obtained by ^{51}V(π^+,K$^+$)$^{51}_{\Lambda}$V reaction with the Moby-Dick spectrometer system at BNL-AGS. Energy resolution is 3 MeV(FWHM) [25].

^{51}V(e,e'K$^+$)$^{51}_{\Lambda}$Ti reaction :

In the ^{51}V target , the neutron $f_{7/2}$ shell is well closed and stable because N=28, while one of the three protons in the f-shell is converted to a Λ hyperon in the bound region. In this hypernuclear mass region, a hyperon is bound up to d-orbital, providing us an opportunity to observe the splitting in the d orbital. The splitting here could be larger because of a factor $l_\Lambda(l_\Lambda + 1)$, which gives us a better chance to directly observe it. The hypernucleus, $^{51}_{\Lambda}$V, was studied by the (π^+, K^+) reaction at BNL with resolution around 3 MeV(FWHM) and it is shown in Fig.6 [25]. The quality of the spectrum is poor but the major shell structure is seen. For the (γ,K$^+$) reaction, a model calculation has been carried out similarly as ^{28}Si(γ,K$^+$)$^{28}_{\Lambda}$Al [37], excitation spectrum of which is shown in Fig.7. Although the calculation is preliminary, it is readily recognized that the spin-orbit partner states both for p and d orbitals are populated with reasonable cross section. The $[\pi f_{7/2}^{-1} \otimes \Lambda d_{5/2}]6^-$ and $[\pi f_{7/2}^{-1} \otimes \Lambda d_{3/2}]5^-$ states, which are spin-orbit partners, are expected to be split by more than 1 MeV if $V_{so} = 2$ MeV. The calculated spectrum suggests that these states will be preferentially populated.

Since nuclei in this mass region are rather well described by shell-model wave functions, it is expected that comparison between experimental data and theoretical calculations will have less ambiguities. We will therefore have a good chance to relate the splitting to the magnitude of spin-orbit splitting in the d orbital.

Although the present proposal emphasizes the importance of spin-orbit splitting in the p and d orbitals, it should be also mentioned that spectroscopic investigation of these hypernuclei with sub-MeV resolution should bring high quality information

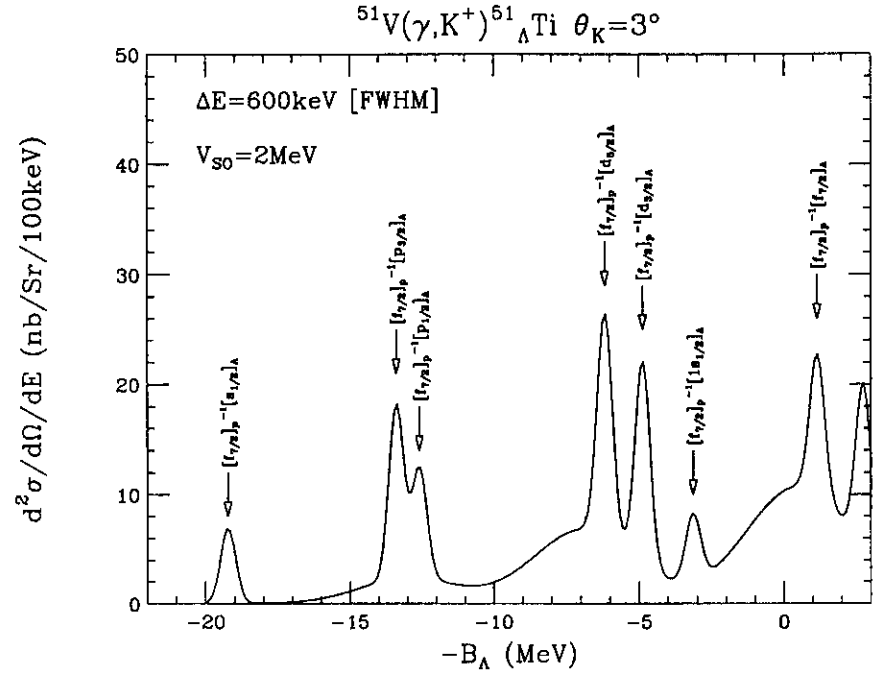

Figure 7: Calculated excitation function of $^{51}V(\gamma,K^+)^{51}_\Lambda Ti$ reaction at E_γ = 1.3 GeV/c and θ_K = 3 deg [37]. Spin-orbit splitting of the *p*, *d* and *f* orbitals is assumed to be 0.8, 1.3 and 1.6 MeV respectively as taken from Fig.3. Contribution from *d* proton-hole states are smeared by 4 MeV.

on the structure of Λ hypernuclei beyond the *p* shell region for the first time.

6 Experiments

In the present proposal, we plan to use the hypernuclear spectrometer system (HNSS) in Hall C. This apparatus will be used for the approved E89-09 experiment, which is under preparation. The spectrometer system consists of

1. the SOS spectrometer which identifies kaons from the target and analyzes their momenta,
2. the Enge split-pole spectrometer which measures scattered electrons, and
3. the Splitter magnet that separates scattered electrons and kaons at extremely forward angles by bending them to a large angle separation.

The details of HNSS can be found in the various documents describing the E89-09 proposal [36]. The latest status of the HNSS is also explained in Appendix A. Figure 8 shows the experimental setup around the target area and the electron spectrometer.

The general arrangement of the experiment is identical to E89-09. We will use an incident beam energy of 1.645 GeV/c. Kaons scattered at 3 degrees with respect to virtual photon direction are detected by the SOS spectrometer. Electrons scattered at 0 degrees are measured with the Enge split pole spectrometer. The splitter deflects the kaons and scattered electrons by +16.4 and -33 degrees with respect to the beam direction (the same as the virtual photon direction),

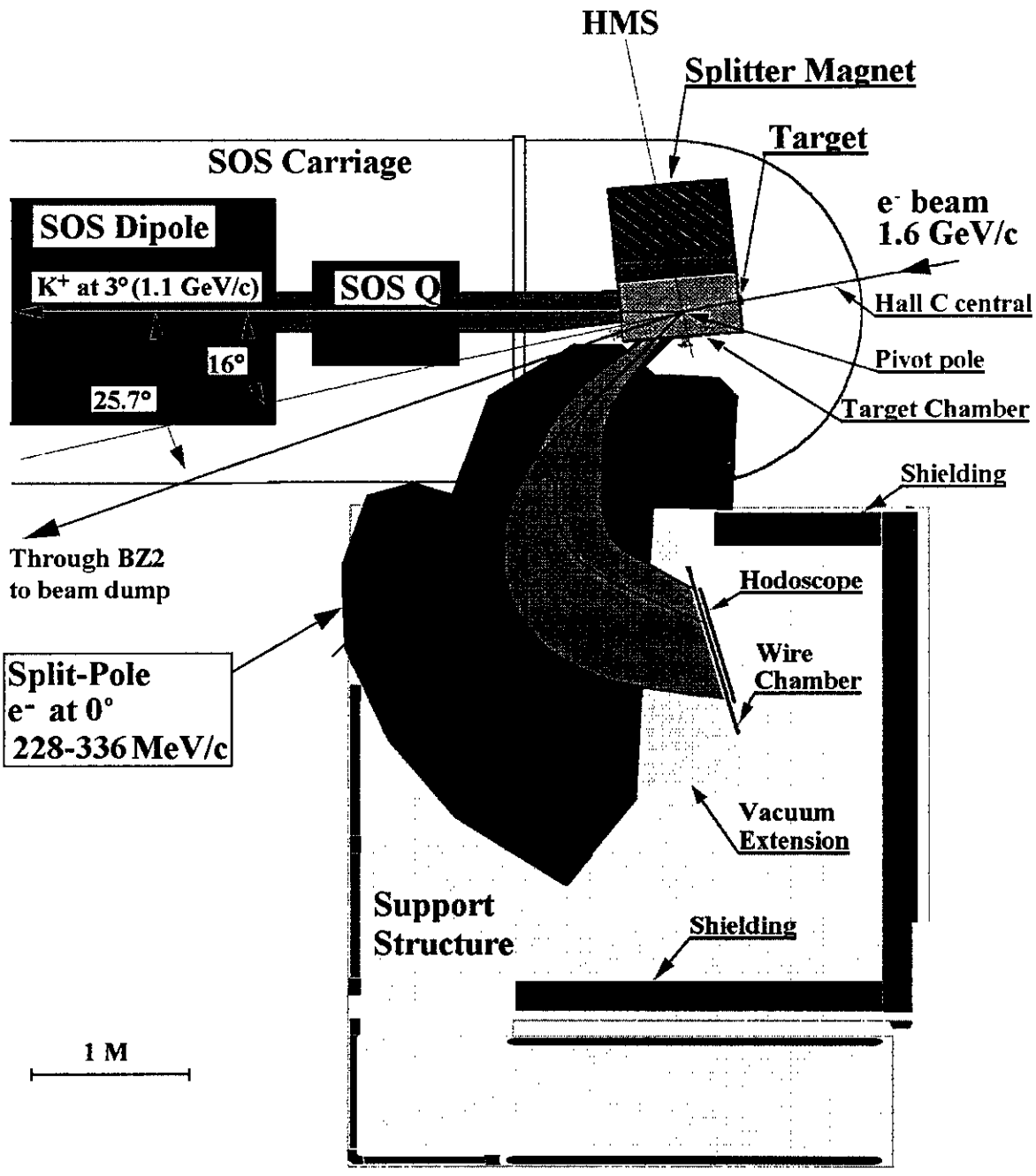

Figure 8: Experimental set-up for the present proposed experiment (Identical with the one for updated E89-09 [36]).

respectively. This geometry maximizes the hypernuclear production thus allowing the use of a low beam current, a low beam energy, and a thin target to achieve the best possible energy resolution. The virtual photon energy will be 1.36 GeV/c.

The intensity of the electron beam is limited by the total count rate of the electron spectrometer, which is dominated by low energy electrons created in the bremsstrahlung process in the target. In order to keep the accidental coincidence rate under control, the maximum intensity integrated over the entire focal plane will be kept under $2 \times 10^{+8}$/sec as in E89-09. The target thickness will be 10 mg/cm^2 in which the energy loss is less than 20 keV, so that this contribution to the energy resolution can be neglected. The maximum acceptable intensity of the beam, estimated to be less than a μA for the proposed targets, is listed in Table 3. The virtual photon flux, and consequently the yield, decreases as inverse of radiation length. The yield per (hr/50nb/sr) is then calculated including a kaon decay factor of 0.4 and overall kaon detection efficiency of 0.8. Cross sections larger than 50 nb/sr are expected for each of the spin-orbit partner states of the Λ p orbital in $^{28}_{\Lambda}$Si and the Λ d orbital in $^{51}_{\Lambda}$V. The result is 2.9/hr/(50nb/sr) for the ^{28}Si target and 1.2/hr/(50nb/sr) for the ^{51}V target. The rate for the ^{51}V target is about one order of magnitude smaller than that of the ^{12}C target estimated for E89-09 but is still large enough to obtain reasonable statistics (more than 500 counts for 50 nb/sr in the requested beam time).

The backgrounds due to positrons, pions, and protons in the SOS spectrometer were estimated by the same prescription given in the E89-09 proposal and summarized in Table 3. The positron single rate was evaluated from the pair production cross section. The pion and proton backgrounds are scaled from the EPC calculation done for the carbon target assuming the $A^{2/3}$ dependence and are shown in table 3. The positron rate is well suppressed in the trigger with the shower counter and the aerogel Cerenkov counter so that an overall positron rejection efficiency of 6×10^{-5} will be obtained. Therefore, the singles rate in the trigger from positrons is well below 1 count/sec.

The SOS kaon identification system, which consists of an aerogel counter, a Lucite counter, the TOF scintillation hodoscopes, and the shower counters, has been already established and was used successfully in the first two experiments using the (e,e'K$^+$) reaction, E91-016 and E93-018. A 20 hour test run using a C target was also conducted during these experiments which demonstrated an excellent performance of the kaon identification system. From the test run, it was learned that the online trigger rate will be less than 10 Hz with more than 10% being kaon triggers. The same is then expected for the HNSS setup of both the proposed experiment and E89-09. The detail of the SOS kaon identification for the test run is described in the Appendix.

The quasifree kaons that will be accepted in the SOS spectrometer were estimated by scaling the virtual photon flux and the quasifree hyperon production cross section. The cross section is assumed to be proportional to $Z^{0.8}$, taking into account the effective proton number for the ^{12}C(γ,K)$^{12}_{\Lambda}$C which was determined experimentally at INS, Tokyo [38]. Since the larger cross sections for the production of kaons are more or less compensated by the less intense beam which we use for the

Table 3: Count rates in the (e,e'K^+) reaction

Target	Rad. Length (cm)	Max.e^- Intensity (μA)	Yield/hr /(50nb/sr)	e^+ in SOS/sec	π^+ in SOS/sec	p in SOS/sec	Qfree K^+ in SOS/sec
^{12}C	42.7	1.6	13.4	6.0 E+3	180	18	0.39
^{28}Si	**21.8**	**0.79**	**2.9**	**3.4 E+3**	**69**	**6.9**	**0.39**
^{51}V	**15.8**	**0.60**	**1.2**	**6.6 E+4**	**41**	**4.1**	**0.42**
^{89}Y	10.4	0.38	0.44	4.3 E+4	23	2.3	0.42
^{139}La	8.1	0.30	0.23	9.9 E+4	15	1.5	0.45
^{208}Pb	6.4	0.23	0.12	2.0 E+4	10	1.0	0.47

heavier targets, the kaon rate in the SOS stays almost constant and about 0.4/sec (see Table 3). This gives an accidental rate of about 0.16/sec taking into account the 2 $\times$ 10^8 scattered electrons/sec and 2 ns coincidence time window. Therefore, the ratio of true kaon over accidental kaon rates within the same 2 ns beam bucket is about 2.5. This ratio in the test run with scattered electrons at about 15 degrees was approximately 0.8 in the first 10 hour run and 1.6 in second 10 hour run with different kinematics. Still, satisfactory extraction of the hypernuclear missing spectra was demonstrated (see the detail in the Appendix).

The momentum resolution of the SOS spectrometer has been confirmed to be better than 9 x 10^{-4}, which was tested using elastic electron scattering of an *Al* target in December of 1996. Unfortunately, the beam spot size at the target during the test run was 10 times worse than normally achieved. Optical studies show that the resolution will be at 5 x 10^{-4} level with a normal beam size of about 0.12 mm FWHM. The electron spectrometer to be installed for E89-09 in Hall C has been used and operated at many laboratories in the world, it has a much better resolution than the SOS spectrometer at 10^{-4} level. A list of the contributions to the momentum resolution from all possible sources is discussed in the Appendix. The overall energy resolution is completely dominated by the SOS spectrometer and expected to be about 600 keV if stable beam is delivered to the target.

7 Requested beamtime and support

We propose to collect at least 500 counts per 50 nb/sr cross section and request a beamtime of 720 hours for data acquisition. It will also take 120 hours to setup for the proposed medium heavy targets. The requested beam time is summarized in Table 4.

We would like to run this experiment without intermission after the E89-09 experiment. Since the experimental setup is identical, we believe that it would be

Table 4: Requested beam time

	Target	number of days	number of hours
Tuning, Calibration		5 days	120
Data taking	^{28}Si	10 days	240
	^{51}V	20 days	480
Total		35 days	**840 hrs**

Table 5: Requested beam conditions

Beam energy	1.645 GeV/c
Beam current	$< 1\ \mu$ A

the most efficient way to run the experiment. The two experiments will share most of the calibration and manpower which will maximize the scientific outcomes. If the proposed experiment does not run immediately after the E89-09 experiment, we request additional time for re-installing and tuning the spectrometer system. It needs about 15 (critical path) days and about \$20K of cost to re-install the HNSS system.

The requested beam conditions are also listed in Table 5.

8 Summary

Recent progress of the Λ hypernuclear spectroscopy with 2 MeV resolution has proved that high resolution spectroscopy has significant value in investigating the structure of Λ hypernuclei and the Λ hyperon-nucleon interaction. It is now evident that Λ hypernuclear spectroscopy by the (e,e'K$^+$) reaction will play a leading role in the Λ hypernuclear spectroscopy because of its high energy resolution, and beam quality. It should be specifically noted that the beam size and thin target samples allow the use of separated isotopes. This is not possible at any other laboratory and allows one a much more extensive choice of targets to optimize the physics output.

In summary, here are the goals of the present proposal:

- We intend to determine the spin-orbit splitting in p and $d-$ Λ orbitals, by taking advantage of the fact that the spin-flip amplitude of the electromagnetic production of Λ hypernuclei is large, and that the expected energy resolution of Hall C HNSS will reach sub-MeV level. The heavier targets, ^{28}Si and ^{51}V, are chosen because we can expect greater spin-orbit splitting.
- We plan to investigate Λ hypernuclear structure in the mass region beyond the p shell up to A $\approx$ 50 with sub-MeV energy resolution.

- Technically, the success in completing the first two (e,e'K^+) experiments, E91-016 and E93-018 in Hall C, as well as the test run with the C target that was performed during these experiments under much more severe condition than both E89-009 and the current proposal, has clearly demonstrated the feasibility to investigate the Λ hypernuclear system beyond the p shell to mass ≈ 50 region or even higher.

This proposal is a part of a larger study of strangeness nuclear physics, supported in part by a US-Japan collaborative research program under the auspices of the US NSF and Japan Society for Promotion of Science(JSPS), and also by Ministry of Education(Monbusho), Japan.

References

[1] H. Bandō, T. Motoba and Y. Yamamoto, Phys. Rev. **C31** 265 (1985).

[2] A. Likar, M. Rosina and B. Povh, Z. Phys. **A324** 35 (1986).

[3] Th.A. Rijken *et al.*, Nucl. Phys.**547** (1992) 245c.

[4] K. Holinde, Nucl. Phys. **A547** (1992) 255c.

[5] Y. Yamamoto and H. Bando, Prog. Theor. Phys. Suppl.**81** (1985) 9.

[6] A. Gal, J.M. Soper and R.H. Dalitz, Ann. Phys. **113** (1978) 79.

[7] D.J. Millener, A. Gal, C.B. Dover and R.H. Dalitz, Phys. Rev. **31** 499 (1985).

[8] V.N. Fetisov, L. Majling, J. Zofka and R.A. Eramzhyan, Z. Phys. **A339** 399 (1991).

[9] T. Hasegawa *et al.*, Phys. Rev. Lett. **74** (1995) 224.

[10] W. Bruckner *et al.*, Phys. Lett. **79B** (1978) 157.

[11] A. Bouyssy, Phys. Lett. **84B** (1979) 41. A. Bouyssy, Phys. Lett. **91B** (1979) 15.

[12] M. May *et al.*, Phys. Rev. Lett. **47** (1981) 1106.

[13] R.H. Dalitz, Nucl. Phys. **A450** (1986) 311c.

[14] A. Bouyssy, Nucl. Phys. A290 (1977) 324.

[15] R. Brockmann and W. Weisse, Phys. Lett. **69B** (1977) 167.

[16] R. Brockmann and W. Weisse, Nucl. Phys. **A355** (1981) 365.

[17] H.J. Pirner, Phys. Lett. **85B** (1979) 190.

[18] O. Morimatsu, S. Ohta, K. Shimizu and K. Yazaki, Nucl. Phys. **A420** (1984) 573.

[19] C.B. Dover and A. Gal, Prog. Part. Nucl. Phys. **Vol. 12** (1984) 171.

[20] R.H. Dalitz, D.H. Davis, T. Motoba and D.N. Tovee, submitted (1997)
T. Motoba, Soryuushiron Kenkyu **Vol. 94, No.2** (1996) B53. Proceedings of Workshop on Hyperon-Nucleon Interaction and Related Topics, Yukawa Institute for Theoretical Physics, Kyoto (March, 1996)

[21] T. Nagae, Proceedings of the 23rd INS international symposium on Nuclear and Particle Physics with Meson Beams in the 1 GeV/c Region, Tokyo, March 15-18, 1995. Eds. S. Sugimoto and O. Hashimoto.

[22] O. Hashimoto, Proceedings of QULEN97, May 20-23, 1997, Osaka. to be published in Nucl. Phys.

[23] M. May *et al.*, Phys. Rev. Lett. **78** (1997) 4343.

[24] BNL-AGS experiment E929, September 1996.(Spokesperson T. Kishimoto)

[25] P. H. Pile *et al.*, Phys. Rev. Lett. **66** 2585 (1991).

[26] T. Hasegawa *et al.*, Phys. Rev. **C53** (1996) 1210.

[27] C.B. Dover, L. Ludeking and G.E. Walker, Phys. Rev. **C22** 2073 (1980).

[28] H. Bandō and T. Motoba, Prog. Theor. Phys. **76** 1321 (1986).

[29] T. Motoba, H. Bandō, R. Wünsch and J. Zofka, Phys. Rev. **C38** 1322 (1988).

[30] O. Hashimoto *et al.* Il Nuovo Cimento **102** 679 (1989).

[31] T. Fukuda *et al.*, Nucl. Instr. Meth. **A361** (1995) 485.

[32] O. Hashimoto, Hyperfine Interactions **103** (1996) 245.

[33] AGS Experiment E907 (Spokespersons E. Hungerford and J.C. Peng)

[34] T. Motoba, M. Sotona and K. Itonaga, Prog. Thor. Phys. Suppl. No. 117 (1994) 123.

[35] T. Motoba and J. Zofka, unpublished (1984)
O. Hashimoto,"Perspectives of Meson Science" p.547, eds. T. Yamazaki, K. Nakai and K. Nagamine, North Holland, 1992.

[36] E. Hungerford *et al.* Proposal to JLAB PAC E89-09 (1989),
Status of Experiment E89-09 and a response to the scheduling review committee (Jan. 1995),
A revised Experimental Geometry for E89-09 which requires less time and is less costly to setup(Mar. 1996)

[37] T. Motoba, unpublished, 1997.

[38] H. Yamazaki *et al.*, Phys. Rev. **C52** (1995) R1157.

Appendix

A. Hall C HNSS Status

The HNSS system is shown in Fig.8. The kaon detection for the SOS spectrometer is well established (see detail in the next section). The splitter magnet has been field mapped and is ready to be commissioned. The Split-pole spectrometer has been modified and tested and is also ready for commissioning. The supporting structures for both the Splitter and Split-pole are constructed and are now stored in the Test Lab at JLAB. They are ready for installation. The Power supply for the Split-pole will be shared with the Moller polarimeter in Hall C. The power supply for the BZ magnet which re-orients the beam back to the dump is purchased and will be available before 1998. A new power supply is needed and will be purchased by Hall C in 1998, which will be able to power the Splitter magnet.

The scintillation hodoscope with 64 strips is under construction and will be completed and tested as a complete unit in the summer of 1997, it will be ready in 1998. The timing resolution was tested to be better than 500ps FWHM which is sufficient for coincidence with kaons from SOS as it distinguishes individual beam buckets. The 2.5/1 ratio of the true kaons over accidental kaons will allow us to easily recognize the real coincidence beam bucket.

The high rate MWPC chamber for the electron arm has been built and tested at BNL. It will have low gas and high electronics gain to match the high rate requirement. To reach the best possible energy resolution, the collaboration is planning to build a Silicon Strip Detector (SSD) which has 0.45 mm pitch width, with rate capability of 10^6 per pitch. In this case, the rate per pitch is about 1.3×10^5. The SSD is capable of running continuously for 1500 hours before a reduction in efficiency to less than 97% due to radiation damage. This device can be ready in one year, and a prototype will be ready for tests by the fall of 1997.

Thus, all the key elements for HNSS will be ready before 1999.

B. The SOS Kaon Identification System

Figure 9 shows the SOS kaon identification system. The particle ID system includes two separated wire chambers (total of 12 planes) for tracking, 4 hodoscope planes as a pair (X and Y direction) and separated by about 1.5 meter, a Lucite total internal reflective Cerenkov counter, an aerogel Cerenkov counter, and shower counters. Figure 10 shows the threshold effect of the Lucite counter obtained from experimental data. The beta of protons is below 0.8 so that a cut at a 3 photoelectron level will reject 90% of protons. The remaining protons are due to large incident angles and can be cleaned by TOF.

A feasibility test run for hypernuclear production was carried out during the E91-016 and E93-018 runs. In the test run, the scattered electrons were detected by the HMS spectrometer at a scattering angle of 14.3 degree which is about the minimum for HMS. To maximize the production, the beam energy was 3.245 GeV and momenta of the scattered electrons were centered at 1.75 GeV/c. Then the

kaons with central momentum of 1.2 GeV/c were detected by SOS at the virtual photon direction which was at the minimum opening angle with respect to HMS. In this setup, both the protons/kaons and pions/kaons ratios are about or higher than 1000, while the kaons are dominantly from quasifree production since the hypernuclear ground state from that setup is at least three order of magnitudes lower than that of 0 degree scattering. With 0.5 g/cm^2 C target and an average beam current of 30 μA, the kaon rate was about 1/sec while the ground state production rate was expected no more than about 1.5/hr. It was demonstrated that the aerogel and Lucite counters reject 95% of pions and 90% of protons at the online level without losing kaons so that the trigger rate was reduced to about 100 Hz. The single arm SOS TOF referred to the RF showed clean separation of kaons from pions, protons, and positrons. Figure 11 shows a comparison of data taken with and without Lucite and aerogel in the trigger. One can see the change in the ratio of kaons over protons and pions.

The TOF is done by the hodoscopes with path length correction and reconstruction to the target using beam RF. Figure 12 shows the single SOS arm TOF spectrum in which the kaons are cleanly singled out from all other background.

Figure 13 shows a two dimensional plot, TOF vs coincidence time. One can see that each individual beam bucket is clearly seen with the real coincident bucket more dense. Figure 14 shows a coincidence spectrum after the TOF cut which cleans away all other background particles except kaons. From this figure one can see that we had about a 1/1 ratio of true kaons over accidental kaons which ensured the recognition of the real coincidence. Accidental background was subtracted by analyzing a number of accidental coincidence beam buckets to minimize the contribution of statistical error due to the subtraction.

Figure 15 shows the overall missing mass spectra for a C target in the test run with two different kinematics and beam currents. The shaded areas are the accidental background. It showed a beam current square dependence on the accidental rate by comparing the two runs with different beam currents. In this test run, both protons and pions were 1000 times more than kaons which were dominant from quasifree production. The cross section was so small that only about 1-2 counts per hour was expected even with about 30 μA beam and 0.5 g/cm^2 target. By combining 8 accidental coincident kaon peaks in the coincidence spectrum, the accidental background shape was then obtained without statistical fluctuation. This background was subtracted from the missing mass spectrum after it was divided by 8. Figure 16 shows a missing mass spectrum in terms of the Λ binding energy in the particle emission region. Although the structure in the data is suggestive, statistics are very low due to an extremely small cross section for the test run setup and short beam time. It is clear however that there is strength in the bound state region which is consistent with the expected value.

C. Energy resolution

The contribution to the overall energy resolution can be broken down from SOS, the beam, Split-pole, the scattering angle uncertainty, and the target energy loss,

Table 1A. Energy resolution

Item	Uncertainty	Contribution
SOS momentum	1.055 GeV/c x ($5x10^{-4}$)	502 keV
Beam momentum	1.645 GeV/c x ($1x10^{-4}$)	165 keV
Enge momentum	0.282 GeV/c x ($2x10^{-4}$)	56 keV
Scattering angle	13 mr FWHM	240 keV (C) $\leq$ 120 keV (Si,V)
Target	10mg/cm^2	17 keV (C) $\leq$ 20 keV (Si,V)
Overall		583 keV (C) 547 keV (Si,V)

they are listed in Table 1A.

The intrinsic SOS momentum resolution was tested by elastic electron scattering from an Al target with thickness about 2% of radiation length. Figure 17 shows the absolute momentum error distribution from the beam momentum. A resolution of $9x10^{-4}$ was obtained. However, an unusually large beam spot size of about 1.2 mm which is an order of magnitude larger than the normal beam spot was used during the short test run due to technical problems in the accelerator during that time. Optical studies reproduced this resolution with this large beam size. Thus, we are confident that the SOS will be able to reach $5x10^{-4}$ resolution if beam quality is normal.

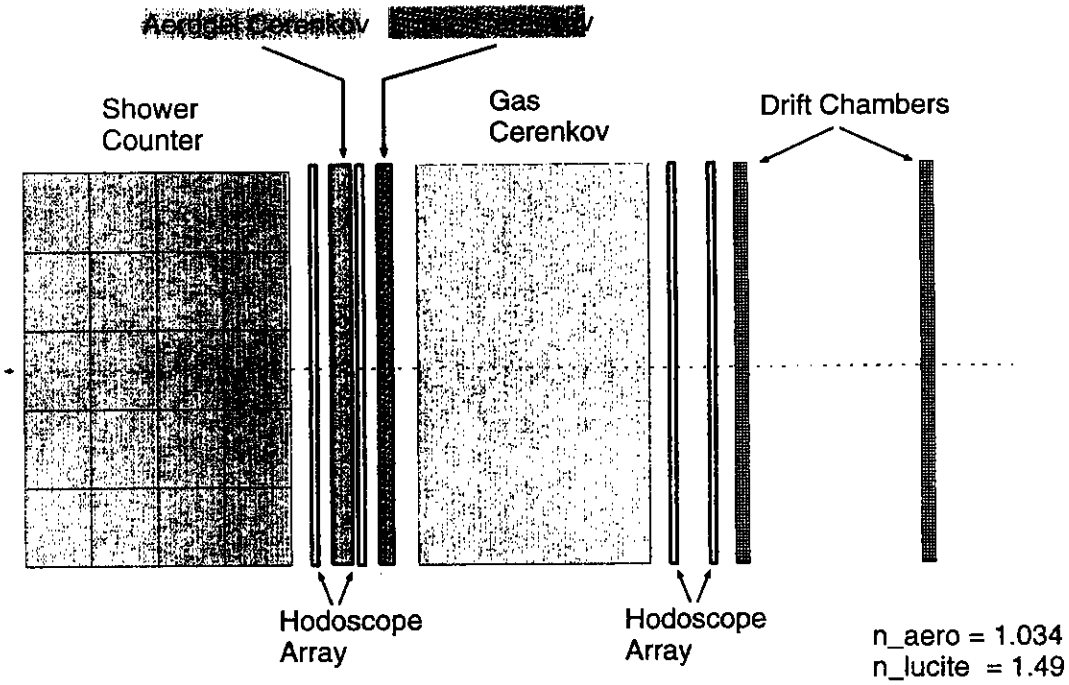

Figure 9: The SOS kaon identification system

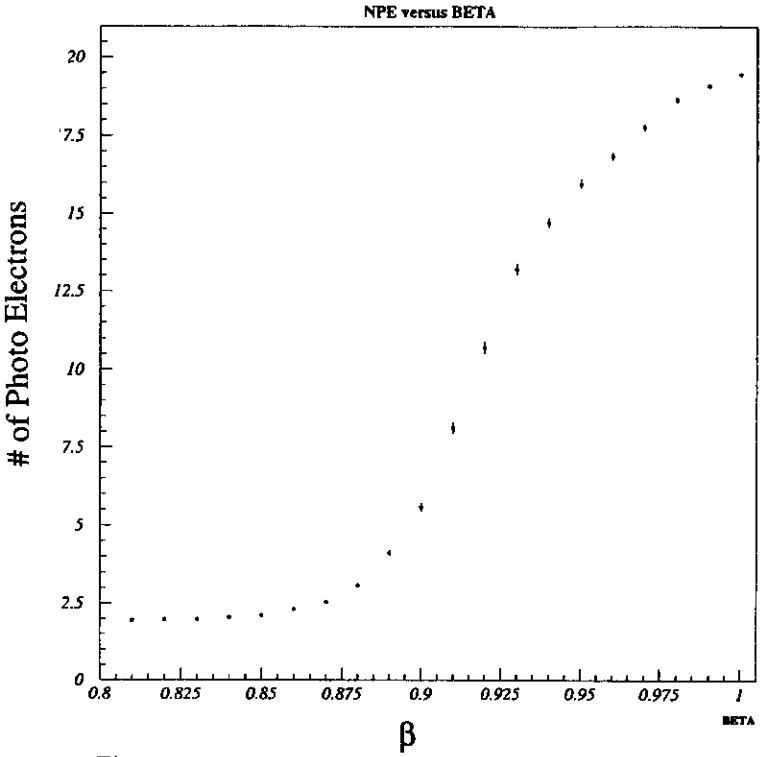

Figure 10: The threshold effect of the Lucite counter

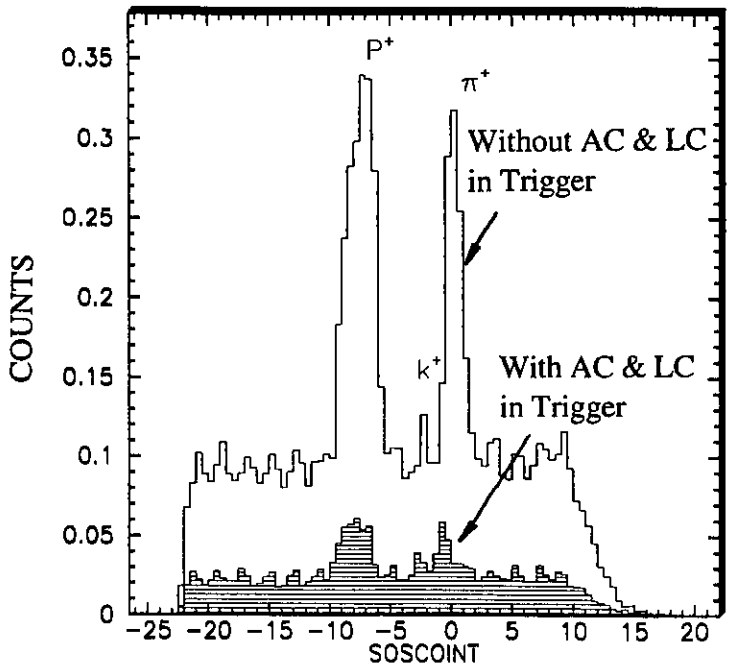

Figure 11: Comparison of data with and without Lucite and aerogel in the trigger

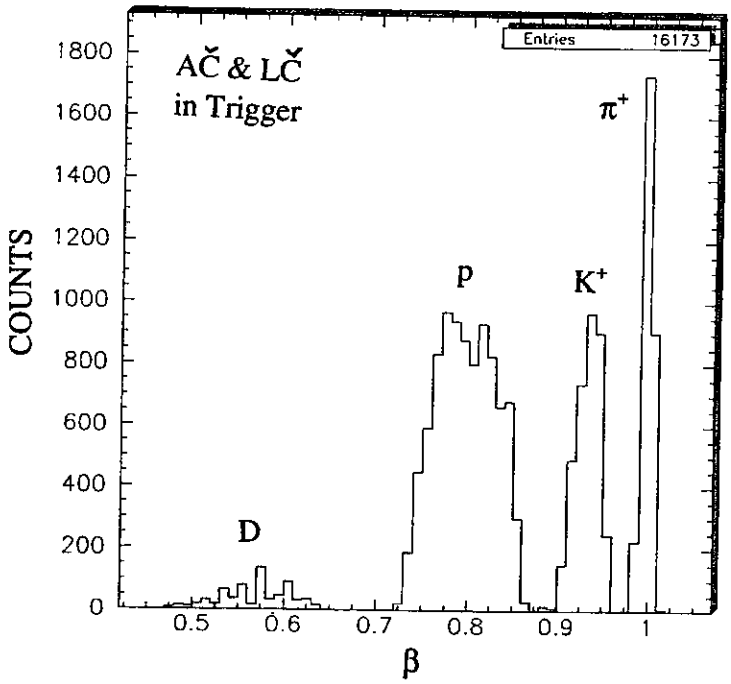

Figure 12: TOF singles spectrum of the SOS spectrometer